

## Model-based estimation of Frank-Starling curves at the patient bedside

Rachel Smith\* J. Geoffrey Chase\* Christopher G. Pretty\*  
Shaun Davidson\*\* Geoffrey M. Shaw\*\*\* Thomas Desai\*\*\*\*

\* Department of Mechanical Engineering, University of Canterbury,  
New Zealand (e-mail: [rachel.smith@pg.canterbury.ac.nz](mailto:rachel.smith@pg.canterbury.ac.nz)).

\*\* Institute of Biomedical Engineering, University of Oxford, United  
Kingdom

\*\*\* Christchurch Hospital Intensive Care Unit, New Zealand

\*\*\*\* IGA Cardiovascular Science, University of Liège, Liège, Belgium

**Abstract:** Determining physiological mechanisms contributing to circulatory failure can be challenging, contributing to the difficulties of delivering effective hemodynamic management in critical care. Measured or estimated Frank-Starling curves could potentially make it much easier to assess patient response to interventions, and thus to manage circulatory failure. This study combines non-additionally invasive model-based methods to estimate left ventricle end-diastolic volume (LEDV) and stroke volume (SV) during hemodynamic interventions in a pig trial. Frank-Starling curves are created using these metrics and Frank-Starling contractility (FSC) is identified as the gradient. Bland-Altman median bias [limits of agreement (2.5th, 97.5th percentile)] are 0.14 [−0.56, 0.57] for model-based FSC agreement with measured reference method FSC using admittance catheter LEDV and aortic flow probe SV. This study provides proof-of-concept Frank-Starling curves could be non-additionally invasively estimated clinically for critically ill patients to provide clearer insight into cardiovascular function than is currently possible.

Copyright © 2021 The Authors. This is an open access article under the CC BY-NC-ND license (<https://creativecommons.org/licenses/by-nc-nd/4.0/>)

**Keywords:** Frank-Starling curves, Hemodynamic monitoring, Intensive care unit, Preload, End-diastolic volume, Stroke volume

### 1. INTRODUCTION

Hemodynamic monitoring is important for diagnosing and managing circulatory failure, a leading cause of intensive care unit (ICU) mortality (Orban et al. (2017)). However, inability to accurately, continuously, and/or non-invasively measure key variables relating to cardiac and vascular function make it challenging for clinicians to elucidate physiological mechanisms contributing to circulatory failure (Desai et al. (2019)).

Frank-Starling curves show the relationship between stroke volume (SV) and preload, and thus contain information regarding cardiac function and contractility. Increases in preload, which can be measured *in vivo* as left ventricle end-diastolic volume (LEDV) (Peverill (2020)), lead to increased SV. This phenomena is caused by the Frank-Starling mechanism, where increased stretch of cardiac muscle prior to contraction causes increased force of contraction (Starling (1918)). The slope of the Frank-Starling curve, Frank-Starling contractility (FSC), is a new construct defined as the extent changes in ventricle filling induce a change in SV. FSC reflects the force-length relationship, and thus contractility, of cardiac muscle. Creating Frank-Starling curves at the patient bedside allows monitoring of how much preload and SV are altered by treatment or changing patient condition, which could further understanding of physiological mechanisms contributing to circulatory failure (Marik (2010)).

This study combines non-additionally invasive methods to estimate LEDV (Davidson et al. (2017)) and SV (Balmer et al. (2020)) to create Frank-Starling curves during hemodynamic interventions in a porcine trial. FSC from model-estimated Frank-Starling curves is validated using directly measured Frank-Starling curves from admittance catheter and aortic flow probe measurements. In a clinical setting, these direct measurements are not feasible. Therefore, the novel non-invasive model-estimated Frank-Starling curves presented would enable much clearer insight into cardiovascular function than is currently possible at the patient bedside.

### 2. METHODS

#### 2.1 Porcine trials and measurements

Pig experiments were conducted at the Centre Hospitalier Universitaire de Liège, Belgium and approved by the Ethics Committee of the University of Liège Medical Faculty, permit number 14-1726.

N=6 pure Piétrain pigs were used, weighing 18.5 kg to 29.0 kg. Pigs were initially sedated and anaesthetised using Diazepam (1 mg kg<sup>−1</sup>) and Zoletil (0.1 mL kg<sup>−1</sup>). Anaesthesia was maintained by sufentanil (0.1 mL kg<sup>−1</sup> h<sup>−1</sup> at 0.005 mg mL<sup>−1</sup>), Thiobarbital (0.1 mL kg<sup>−1</sup> h<sup>−1</sup>) and Nim-bex (1 mL kg<sup>−1</sup> h<sup>−1</sup> at 2 mg mL<sup>−1</sup>), delivered via superior vena cava catheter. Pigs were mechanically ventilated via

tracheostomy using a GE Engstrom CareStation mechanical ventilator (GE 92 Healthcare, Waukesha, WI, USA).

Data were acquired at 250 Hz using Notocord (Instem, Croissy-sur-Seine, France). Signals include blood pressure in the proximal aorta ( $P_{ao}$ ), femoral artery ( $P_{fem}$ ), and vena cava ( $P_{cv}$ ) using high fidelity pressure catheters (Transonic, Ithaca, NY, USA); left ventricle pressures and volumes ( $V_{LV}$ ) using micromanometer-tipped admittance catheters (Transonic Scisense Inc., Ontario, Canada); and aortic flow ( $Q_{ao}$ ) using an ultrasonic flow probe on the proximal aorta (Transonic, Ithaca, NY, USA). All signals were filtered with a 5<sup>th</sup> order Butterworth low-pass filter, with a cut-off frequency of 20 Hz ( $P_{fem}$ ,  $P_{ao}$ ,  $P_{cv}$ ) and 10 Hz for noisier signals ( $V_{LV}$ ,  $Q_{ao}$ ).

Pigs underwent several intervention types: respiratory recruitment manoeuvres (RM) in which PEEP is increased in steps of 5 cmH<sub>2</sub>O to PEEP of  $\geq 15$  cmH<sub>2</sub>O to reduce systemic venous return and thus SV; fluid infusions of 500 mL of saline solution over 30 min to increase circulatory volume and ventricle preload; and an infusion of E. Coli lipopolysaccharide (0.5 mg kg<sup>-1</sup> over 30 minute) to produce a septic shock like response.

Fig 1 shows the order of interventions and data used for each pig. Pig 6 RM 1 was not used due to faulty  $V_{LV}$  readings during the RM. Pigs 1, 3, and 6 died during the endotoxin infusion. The model was calibrated during 10 beats of stable hemodynamics for each intervention, and the ability of model-based estimates to track changes in response to each intervention was assessed.

## 2.2 Measurement of LEDV and SV for validation

Measured SV ( $SV_{mea}$ ) is used for validation and calibration as measured from integrating an aortic flow probe signal ( $Q_{ao}$ ) over one beat for Pigs 2-6. For Pig 1, admittance catheter  $V_{LV}$  is used to obtain SV as the range of  $V_{LV}$  over one beat, due to non-physiological flow probe  $Q_{ao}$  for this pig. Measured LEDV ( $LEDV_{mea}$ ) was calculated from an admittance catheter as the maximum  $V_{LV}$  of each beat.

## 2.3 Non-additionally invasive LEDV estimation

LEDV was estimated from  $P_{mea}$  and heart rate ( $HR$ ) using a method from Davidson et al. (2017), which uses the end-systolic pressure-volume relation (Sagawa (1981)):

$$P_{es} = E_{es} \times (V_{es} - V_0) \quad (1)$$

where  $P_{es}$  is ventricle end-systolic pressure,  $E_{es}$  is end-systolic elastance,  $V_{es}$  is ventricle end-systolic volume, and  $V_0$  is ventricle volume at zero pressure. These terms are made clinically identifiable using:

- $P_{es}$  is estimated as  $P_{es,mea}$ , the end-systole  $P_{mea}$  pressure.  $P_{fem}$  is used for input  $P_{mea}$ , except Pig 4 where  $P_{ao}$  is used due to faulty  $P_{fem}$  measurements. This approach assumes the arterial catheter site for  $P_{mea}$  is sufficiently near the heart that there is negligible pressure drop.
- $V_0$  is replaced with  $V_d$ , ventricle dead space, as these terms are often used interchangeably and have similar physiological values (Sagawa (1981)).  $V_d$  is estimated to be 0.48  $V_{es}$  (Davidson et al. (2017)).

- $E_{es}$  is modelled as  $E_c \times HR^3$ .  $HR$  is used as an indicator of  $E_{es}$  changes.  $E_c$  is a constant, identified through calibration, representing subject-specific coupling between  $HR$  and  $E_{es}$  (Davidson et al. (2017)). This formula is used because  $HR$  changes are typically mathematically sympathetic with  $E_{es}$  changes, as regulatory mechanisms, such as the neural regulatory baroreflex, act on both, rather than each independently (Hall and Guyton (2016)).

Hence,  $V_{es,est}$  can be found from Equation 1 using these surrogate terms (Davidson et al. (2017)):

$$V_{es,est} = \frac{P_{es,mea}}{E_c \times HR^3} + V_d \quad (2)$$

Finally, LEDV is calculated as the sum of  $SV_{est}$  and  $V_{es}$ :

$$LEDV_{est} = V_{es,est} + SV_{est} \quad (3)$$

## 2.4 Non-additionally invasive SV estimation

SV is estimated from the 3-element windkessel model implementation in Balmer et al. (2020). This pulse-contour model relates pressure and flow in the arteries using 3 lumped parameters ( $Z$ ,  $R$ ,  $C$ ) representing resistance and compliance of the systemic circulation. The model estimates  $Q_{ao}$ , and thus SV, from an input arterial pressure signal ( $P_{mea}$ ), and the downstream venous pressure, assumed equal to the average  $P_{cv}$  of each beat ( $\bar{P}_{cv}$ ). The model parameters are identified each beat as an optimisation problem by enforcing the condition of zero flow into the aorta during diastole, as in Balmer et al. (2020).

## 2.5 Calibration

$SV_{est}$  and  $LEDV_{est}$  are calibrated during 10 beats of stable recording at the beginning of each intervention for each pig using  $SV_{mea}$  and  $LEDV_{mea}$ , with the exception of Pig 4 fluid interventions, and the first fluid intervention for Pigs 2 and 3. These interventions are calibrated at the end because fluid administrations began during unstable hemodynamics with rapidly changing blood pressure following the RMs. Parameters identified from calibration are used for the remaining beats of each intervention. Clinically, calibration  $SV_{mea}$  and  $LEDV_{mea}$  could be obtained non-invasively using echocardiography.

The process for model-based SV and LEDV estimation is summarised in Figure 2.

## 2.6 Analysis

Averaged  $SV_{mea}$  and  $SV_{est}$  for each step of each intervention type,  $\bar{SV}_{mea}$  and  $\bar{SV}_{est}$ , are calculated. For RMs, average SV at each PEEP level is found. For fluid infusions, the final 50 beats of each 100 ml portion of the infusion are averaged. For endotoxin infusions and shock, 50 beats are averaged at 5 time points spread evenly across the duration of the 30 minute infusion (Pigs 2,4,5), or from the beginning of the infusion until death (Pigs 1,3,6).  $\bar{LEDV}_{mea}$  and  $\bar{LEDV}_{est}$  are identified in the same manner as for  $\bar{SV}$ . Averaging of LEDV and SV in this manner aims to reduce noise corresponding to LEDV and SV changes not caused by the intervention.

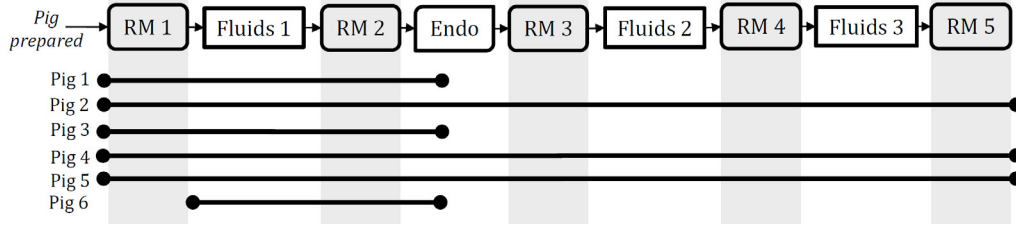


Fig. 1. Time-schedule of experimental interventions and data used for each pig. Interventions are respiratory recruitment manoeuvres (RM), saline solution fluid infusions (Fluids), and an endotoxin infusion (Endo).

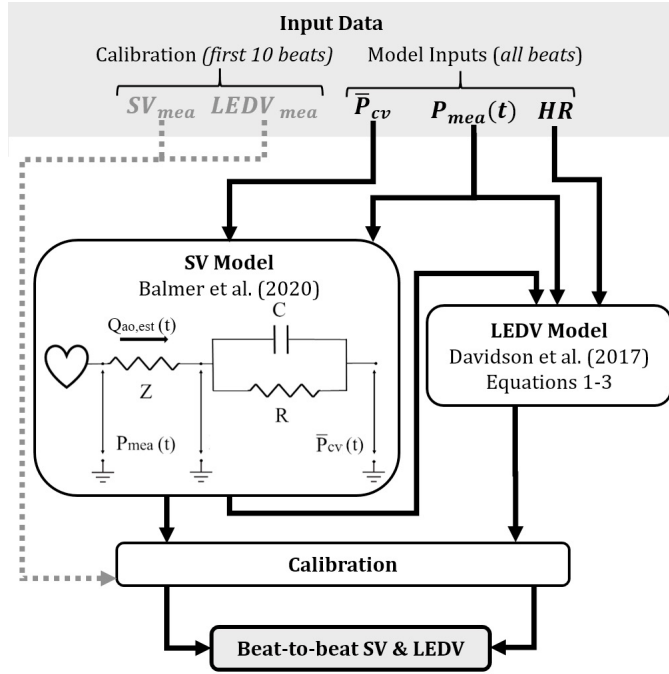


Fig. 2. Overview of model-based SV & LEDV estimation. Model inputs are typically available ICU measures: arterial pressure waveform ( $P_{mea}$ ), beat-wise average central venous pressure ( $\bar{P}_{cv}$ ), and HR. A short period of calibration SV and LEDV values are also required. Models provide beat-beat calibrated estimates of SV & LEDV.

For each pig and intervention a Frank-Starling plot of  $\overline{LEDV}_{mea}$  vs.  $\overline{SV}_{mea}$  and  $\overline{LEDV}_{est}$  vs.  $\overline{SV}_{est}$  was created. In each case a linear-least-squares line of best fit for the  $\overline{LEDV}$ - $\overline{SV}$  relationship was identified. The coefficient of determination ( $R^2$ ) is used to measure goodness of fit to a linear model with an acceptable  $R^2$  defined as  $R^2 \geq 0.75$ . Bland-Altman analysis was used to assess the agreement of model-based and measured slope of the line of best fit, FSC, using Altman and Bland (1983).

### 3. RESULTS

Measured and model-based  $\overline{SV}$  and  $\overline{LEDV}$  responses to each intervention type are shown in Figure 3. Figure 4 shows measured and model-based Frank-Starling curves for each pig. FSC and  $R^2$  from the line of best fit for each intervention are given in Table 1. Figure 5 shows the Bland-Altman agreement of  $FSC_{est}$  and  $FSC_{mea}$ , with median bias and limits of agreement of 0.14 [-0.56, 0.57].

Table 1. FSC and  $R^2$  from line of best fit for measured and estimated Frank-Starling curves for each pig and intervention.

\* indicates  $R^2$  does not meet acceptance criterion of  $R^2 \geq 0.75$

Intervention		FSC		$R^2$	
		<i>mea</i>	<i>est</i>	<i>mea</i>	<i>est</i>
Pig 1	RM 1	0.50	0.57	0.99	1.00
	Fluids 1	0.50	0.25	0.99	0.99
	RM 2	0.49	0.62	0.99	0.99
	Endo	0.34	0.52	1.00	1.00
Pig 2	RM 1	0.98	0.58	0.66*	1.00
	Fluids 1	0.06	0.38	0.08*	0.93
	RM 2	0.65	0.56	0.97	0.97
	Endo	0.78	0.31	0.84	0.98
	RM 3	0.36	0.50	0.75	0.94
	Fluids 2	0.62	0.47	0.73*	0.60*
	RM 4	0.36	0.49	0.86	0.86
	Fluids 3	0.55	0.33	0.75	0.68*
Pig 3	RM 5	0.46	0.62	1.00	0.90
	RM 1	0.28	0.75	0.85	1.00
	Fluids 1	0.24	0.57	0.1*	1.00
	RM 2	0.32	0.79	0.97	1.00
Pig 4	Endo	0.42	0.57	0.97	1.00
	RM 1	0.93	0.59	1.00	0.99
	Fluids 1	0.20	0.37	0.89	0.95
	RM 2	0.60	0.54	1.00	0.97
	Endo	0.27	0.43	0.74*	0.90
	RM 3	0.82	0.61	1.00	1.00
	Fluids 2	0.64	0.49	0.83	0.54*
	RM 4	1.16	0.61	0.96	0.88
Pig 5	Fluids 3	0.99	0.48	0.96	0.95
	RM 5	0.88	0.46	1.00	0.95
	RM 1	0.27	0.53	1.00	1.00
	Fluids 1	0.26	0.39	0.91	1.00
	RM 2	0.31	0.57	0.75	1.00
	Endo	0.45	0.53	0.99	0.96
	RM 3	0.21	0.56	0.83	1.00
	Fluids 2	0.48	0.35	0.98	0.98
Pig 6	RM 4	0.14	0.71	0.60*	0.93
	Fluids 3	0.44	0.58	0.75	0.98
	RM 5	0.19	0.59	0.74*	0.83
	Fluids 1	0.23	0.31	0.95	0.96
Pig 6	RM 2	0.21	0.59	0.97	0.93
	Endo	0.17	0.42	0.76	0.92

### 4. DISCUSSION

#### 4.1 Response to interventions

RMs led to a reduction in  $\overline{SV}$  and  $\overline{LEDV}$ , the extent of which differed between pigs (Fig 3). Fluid infusions increased  $\overline{SV}$  and  $\overline{LEDV}$  at first, then plateaued, and the extent of the increase varied between pigs (Fig 3). Endotoxin infusion and ensuing shock reduced  $\overline{SV}$  and  $\overline{LEDV}$  for all pigs, with different trajectories for each pig

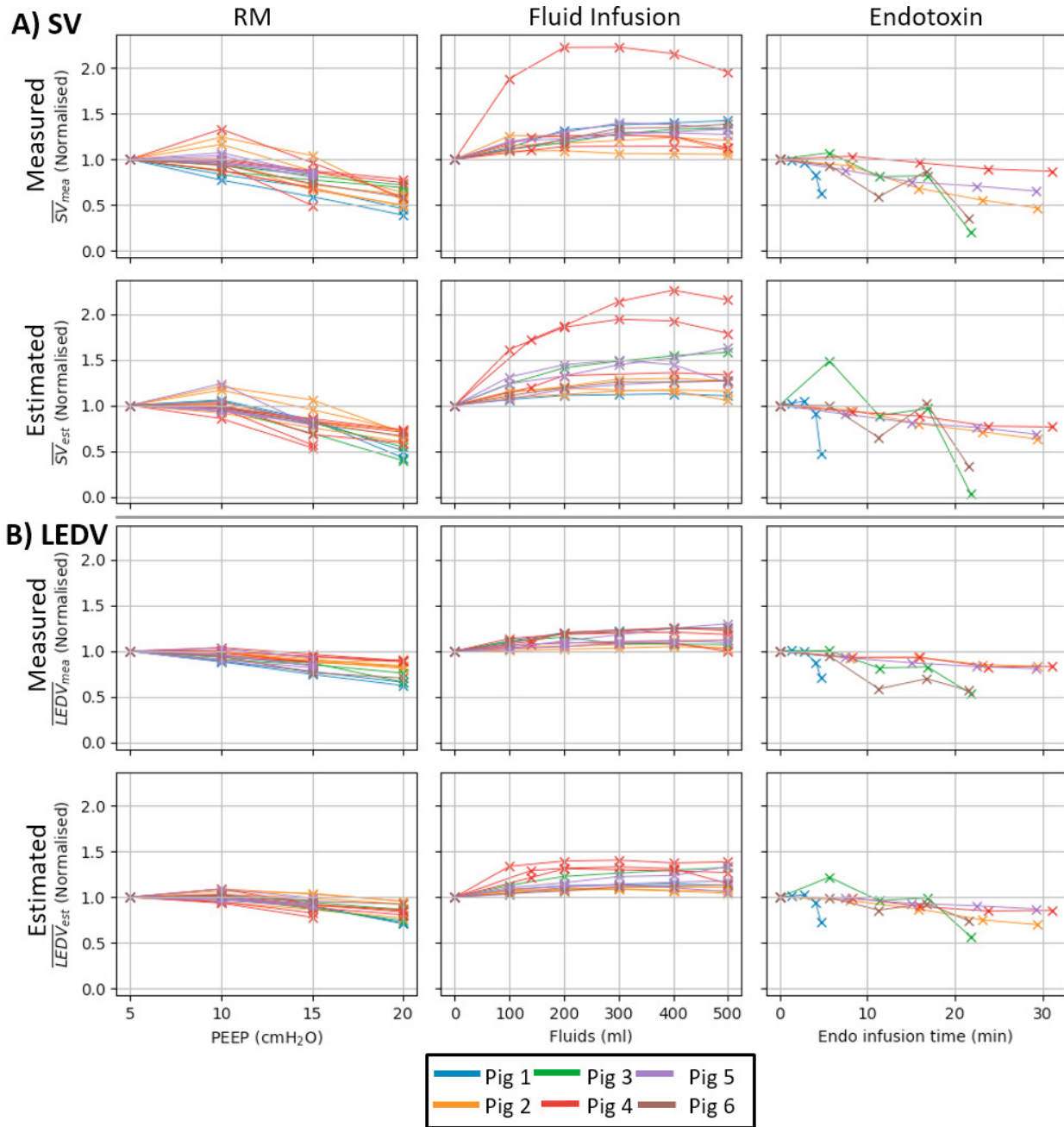


Fig. 3.  $\overline{SV}_{mea}$ ,  $\overline{SV}_{est}$ ,  $\overline{LEDV}_{mea}$ , and  $\overline{LEDV}_{est}$  responses for each intervention type for all pigs. LEDVs and SVs are normalised using the mean value from the first step of each intervention, and thus have no units.

(Fig 3). All responses and variability between pigs matched expectation.

#### 4.2 Frank-Starling curves

A linear model for the  $\overline{LEDV}_{mea}$ - $\overline{SV}_{mea}$  relationship was acceptable ( $R^2 \geq 0.75$ ) for 31 of 38 interventions (Table 1). This linearity meets expectations (Glomer et al. (1985); Wiersema and Bihari (2017)). Thus, it is reasonable to characterise the Frank-Starling relationship using FSC, the gradient of a linear model. Interventions not meeting the criterion ( $R^2 \geq 0.75$ ) were either marginal cases near to the cut-off value, or had very poor  $R^2$  values because the intervention failed to induce a hemodynamic change, resulting in small/negligible change in LEDV/SV

compared to measurement precision. SV is derived from flow probes, quoted as having precision of  $\pm 2\%$  (Yang et al. (2013)) and admittance catheter LEDV has Bland-Altman mean bias [limits of agreement (1.96 standard dev.)] of -5.6 ml [-18.5, 7.3] using 3D echocardiography as a reference method (Kutty et al. (2013)).

Model-estimated FSC had low bias but wide limits of agreement 0.14 [-0.56, 0.57] (Fig. 5). High errors for FSC typically were interventions where  $\overline{LEDV}/\overline{SV}$  responses were small compared to LEDV/SV measurement precision, making it challenging to identify FSC. The limited sample of interventions/pigs makes it challenging to reliably assess the accuracy and precision of FSC estimation.

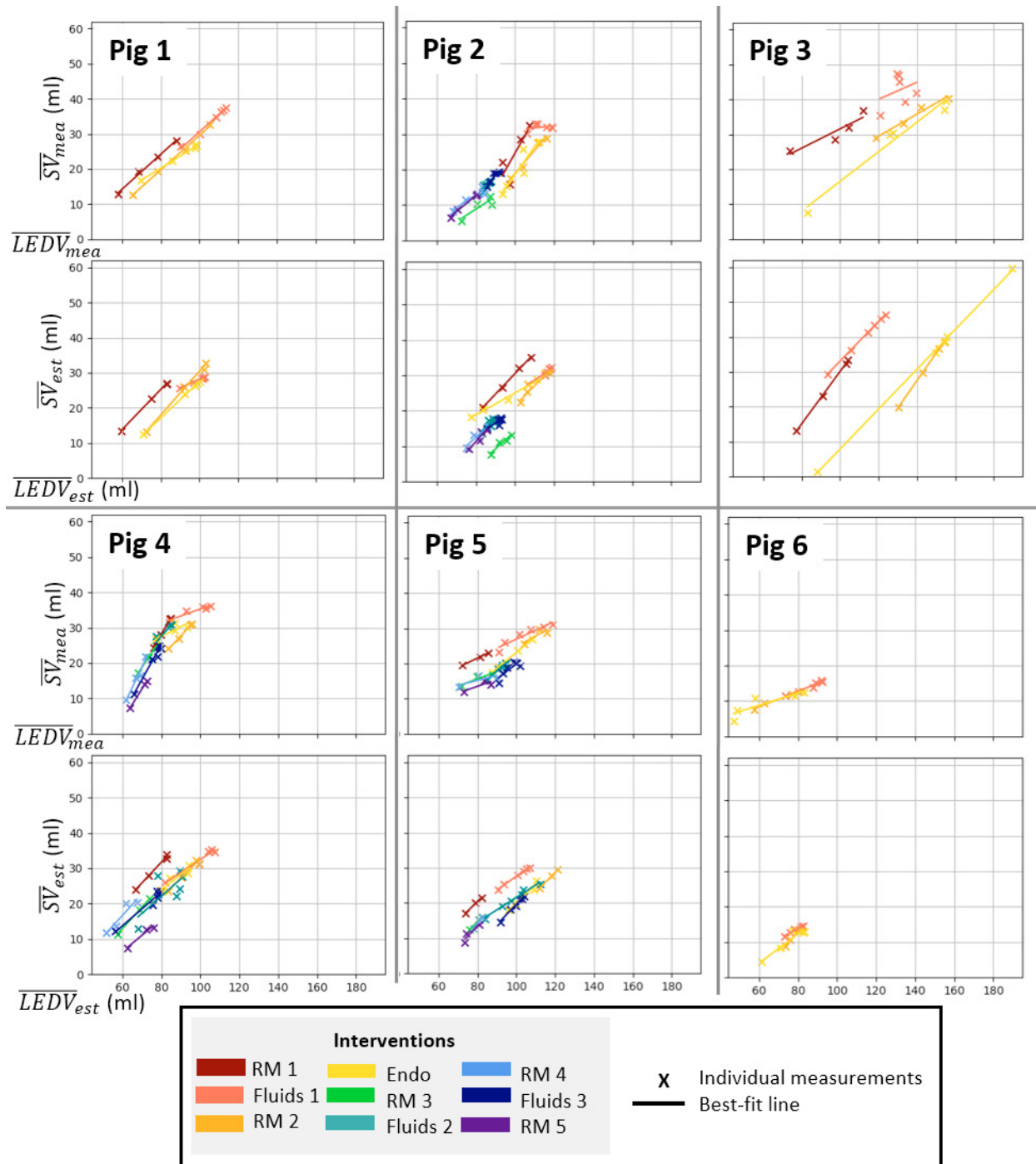


Fig. 4. Frank-Starling plots for each pig using  $\overline{LEDV}_{mea}$  vs.  $\overline{SV}_{mea}$  (upper) and  $\overline{LEDV}_{est}$  vs.  $\overline{SV}_{est}$  (lower).

Clinically, FSC could be used to characterise cardiac muscle performance, as it reflects the force-length relation, and thus contractility, of cardiac muscle. For an intervention inducing a known change in LEDV, FSC could be used to predict and control SV changes, a "holy-grail" of hemodynamic management (Desaive et al. (2019)).

#### 4.3 Limitations

A controlled pig trial differs from critically ill patients, due to anatomical differences between porcine and human cardiovascular systems (Lelovas et al. (2014)), higher fidelity pressure catheter signals than typical clinically, and

a limited number of intervention types which may not reflect all physiological conditions seen in ICU. However, the controlled pig trial enables invasive validation measurements of SV and LEDV, and severe interventions not feasible in a clinical scenario, all of which are useful for validating this method. Thus, these data provide a robust validation set, where the results presented justify further optimisation and validation with human data.

The models used are simple, lumped parameter models, which do not account for spatially varying information. As a result they will not capture all complex phenomena contributing to circulatory pressure-volume relationships.



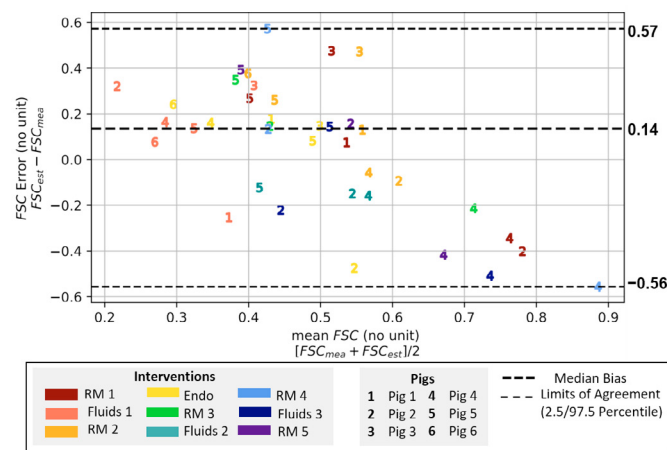


Fig. 5. Bland-Altman plot showing agreement of measured and estimated FSC.

However, the models chosen require fewer inputs while still delivering acceptable accuracy/precision (Balmer et al. (2020)). Note, the methodology used in this study to create Frank-Starling curves, and thus find  $FSC_{est}$ , could be applied to other clinically applicable measures of LEDV and SV.

## 5. CONCLUSION

This study provides proof-of-concept Frank-Starling curves could be estimated at the patient bedside. For a pig trial during hemodynamic interventions, model-based LEDV and SV estimation were used to produce Frank-Starling curves, and thus estimate Frank-Starling contractility, FSC. The non-additionally invasive model-estimated Frank-Starling curves presented could potentially provide clinicians with more insight into physiological mechanisms contributing to circulatory failure, and efficacy of treatment, at the patient bedside.

## ACKNOWLEDGEMENTS

This study was supported with funding from the University of Canterbury Doctoral Scholarship

## REFERENCES

Altman, D.G. and Bland, J.M. (1983). Measurement in Medicine: The Analysis of Method Comparison Studies. *The Statistician*, 32(3), 307. doi:10.2307/2987937.

Balmer, J., Pretty, C.G., Davidson, S., Mehta-Wilson, T., Desaive, T., Smith, R., Shaw, G.M., and Chase, J.G. (2020). Clinically applicable model-based method, for physiologically accurate flow waveform and stroke volume estimation. *Comput Meth Prog Bio*, 185, 105125. doi:10.1016/j.cmpb.2019.105125.

Davidson, S., Pretty, C., Pironet, A., Kamoi, S., Balmer, J., Desaive, T., and Chase, J.G. (2017). Minimally invasive, patient specific, beat-by-beat estimation of left ventricular time varying elastance. *BioMedical Engineering OnLine*, 16(1). doi:10.1186/s12938-017-0338-7.

Desaive, T., Horikawa, O., Ortiz, J.P., and Chase, J.G. (2019). Model-based management of cardiovascular failure: Where medicine and control systems

converge. *Annu Rev Control*, 48, 383–391. doi: 10.1016/j.arcontrol.2019.05.003.

Glomer, D.D., Spratt, J.A., Snow, N.D., Kabas, J.S., Davis, J.W., Olsen, C.O., Tyson, G.S., Sabiston, D.C., and Rankin, J.S. (1985). Linearity of the frank-starling relationship in the intact heart: the concept of preload recruitable stroke work. *Circulation*, 71(5), 994–1009. doi:10.1161/01.cir.71.5.994.

Hall, J.E. and Guyton, A.C. (2016). *Guyton and Hall textbook of medical physiology*. Elsevier.

Kutty, S., Kottam, A.T., Padiyath, A., Bidasee, K.R., Li, L., Gao, S., Wu, J., Lof, J., Danford, D.A., Kuehne, T., and et al. (2013). Validation of admittance computed left ventricular volumes against real-time three-dimensional echocardiography in the porcine heart. *Exp. Physiol.*, 98(6), 1092–1101. doi: 10.1113/expphysiol.2012.070821.

Lelovas, P.P., Kostomitsopoulos, N.G., and Xanthos, T.T. (2014). A comparative anatomic and physiologic overview of the porcine heart. *J. Am. Assoc. Lab. Anim. Sci.*, 53(5), 432–438.

Marik, P.E. (2010). Hemodynamic parameters to guide fluid therapy. *Transfusion Alternatives in Transfusion Medicine*, 11(3), 102–112. doi:10.1111/j.1778-428x.2010.01133.x.

Orban, J.C., Walrave, Y., Mongardon, N., Allaouchiche, B., Argaud, L., Aubrun, F., Barjon, G., Constantin, J.M., Dhonneur, G., Durand-Gasselin, J., Dupont, H., Genestal, M., Goguy, C., Goutorbe, P., Guidet, B., Hyvernat, H., Jaber, S., Lefrant, J.Y., Mallédant, Y., Morel, J., Ouattara, A., Pichon, N., Guérin Rorbardey, A.M., Sirodot, M., Theissen, A., Wiramus, S., Zieleskiewicz, L., Leone, M., Ichai, C., and AzuRea (2017). Causes and Characteristics of Death in Intensive Care Units. *Anesthesiology*, 126(5), 882–889. doi: 10.1097/ALN.0000000000001612.

Peverill, R.E. (2020). Understanding preload and preload reserve within the conceptual framework of a limited range of possible left ventricular end-diastolic volumes. *Adv Physiol Educ*, 44(3), 414–422. doi: 10.1152/advan.00043.2020.

Sagawa, K. (1981). The end-systolic pressure-volume relation of the ventricle: definition, modifications and clinical use. *Circulation*, 63(6), 1223–1227. doi: 10.1161/01.cir.63.6.1223.

Starling (1918). The linacre lecture on the law of the heart given at cambridge, 1915. *Nature*, 101(2525), 43–43. doi: 10.1038/101043a0.

Wiersema, U.F. and Bihari, S. (2017). The frank-starling curve is not equivalent to the fluid responsiveness curve. *Crit Care Med*, 45(3), e335–e336. doi: 10.1097/ccm.0000000000002201.

Yang, X.X., Critchley, L.A., Rowlands, D.K., Fang, Z., and Huang, L. (2013). Systematic error of cardiac output measured by bolus thermodilution with a pulmonary artery catheter compared with that measured by an aortic flow probe in a pig model. *J. Cardiothorac. Vasc. Anesth.*, 27(6), 1133–1139. doi: 10.1053/j.jvca.2013.05.020.